JOURNAL OF AIRCRAFT
Vol. 47, No. 1, January–February 2010

Near-Optimal Trajectories to Manage Landing Sequence in the Vicinity of Controlled Aerodromes

S. M. Malaek* and S. Y. Nabavi†
Sharif University of Technology, 11365-8639 Tehran, Iran

DOI: 10.2514/1.44399

A comprehensive approach is proposed to manage landing sequences and their associated trajectories for an arbitrary number of aircraft in the vicinity of a controlled aerodrome. The current approach, similar to that of "first come, first served," could consider different types of priorities as well as emergencies. The approach is especially useful to combine unstructured free-flight trajectories with structured ones during the approach phase of the flight. A comprehensive cost function considers the relative size of all aircraft together with their relative speeds and flight directions. This helps optimize the amount of fuel consumption while respecting separation minima. Resulting trajectories consist of combinations of arcs and straight lines and are easy for a pilot or controller to follow. We also use the so-called genetic algorithm together with a graphical interface to solve for the optimum solution for different scenarios in an offline manner. A lookup table or an equivalent neural network might also be used to provide quick solution for real-time applications.

Nomenclature

a_{mid} = normal deceleration
$a_{\max}$ = maximum deceleration
C_D = drag coefficient
C_L = lift coefficient
$\mathrm{Cost}|_{\mathrm{FQ}}$ = cost of flight quality
$\mathrm{Cost}|_{\mathrm{Time}}$ = cost of spatial separation
$\mathrm{Cost}|_{\delta t_{i,j}}$ = cost of time separation between ith and jth aircraft
$\mathrm{Cost}|_{\delta x}$ = total cost of spatial separation
$\mathrm{Cost}|_{\delta x}(i, j)$ = cost of spatial separation between ith and jth aircraft
c_i = specific fuel consumption of ith aircraft
d_i = ith straight distance
D = drag
$e_i(\mathrm{man})$ = dissatisfaction factor due to the maneuver
$FP_i(\mathrm{man})$ = failure probability due to the maneuver
$FP_i(\delta t_{i,j})$ = failure probability due to time
g_0 = gravity constant
k_i = importance factor for ith aircraft
L = lift
$L|_{\mathrm{Aircraft}}$ = price of ith aircraft
L_f = price of fuel
m = mass
N_i = number of passengers of ith aircraft
n = number of aircraft
$P(\delta x|_{i,j})$ = conflict probability between ith and jth aircraft
P_f = final position
$P_{i,0}$ = ith initial position, $(X_{i,0}, Y_{i,0})$
$P_{i,1}$ = ith position after straight flight, $(X_{i,1}, Y_{i,1})$
$P_{i,2}$ = ith final position, $(X_{i,2}, Y_{i,2})$
P_0 = initial position
R_i = ith turn radius
T = thrust
TD_i = ith turn direction
T_a = assigned time of arrival
T_e = expected time of arrival
t_i = flight time of ith aircraft
v_w = wind velocity
(X_{c_i}, Y_{c_i}) = ith turn center
(X^{P_f}, Y^{P_f}) = coordinates of P_f
x, y = aircraft position
α = angle of attack
$\Delta\psi_i$ = ith turn angle
γ = heading angle
v = aircraft velocity
φ_{mid} = normal bank angle
$\varphi_{\max}$ = maximum bank angle
ψ = heading angle
ψ_f = final heading angle
$\psi_{i,0}$ = ith initial heading
$\psi_{i,1}$ = ith final heading
ψ_0 = initial heading angle

I. Introduction

THE growth of aerial transportation and its associated delays continue to be a challenge for air traffic specialists. As an example, the total aircraft activities at airports in the U.S. airspace are predicted to have an average annual growth of about 2% until 2020 [1]. The share associated with the commercial traffic is slightly more than average and it amounts to as much as 2.3%. It is also expected that air taxi services experience a similar growth as well. Considering the cost incurred due to the congestion of air traffic and its associated delays, which has been estimated as \$10 billion from 1998 to 2000 in Europe alone [2], one might easily recognize the importance of proper air traffic management (ATM) techniques. In fact, such cost is

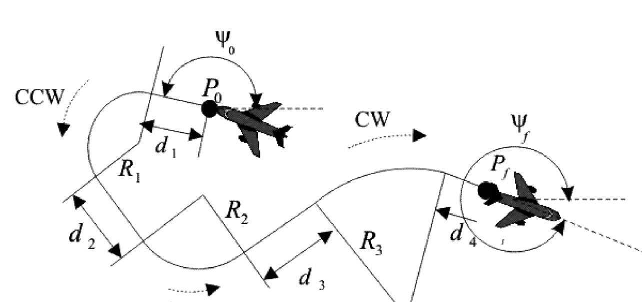

Fig. 1 A typical trajectory based on Dubin, connecting P_0 to P_f.

Received 16 March 2009; revision received 25 July 2009; accepted for publication 31 July 2009.

*Professor, Aerospace Engineering Department.
†Research Assistant, Aerospace Engineering Department.

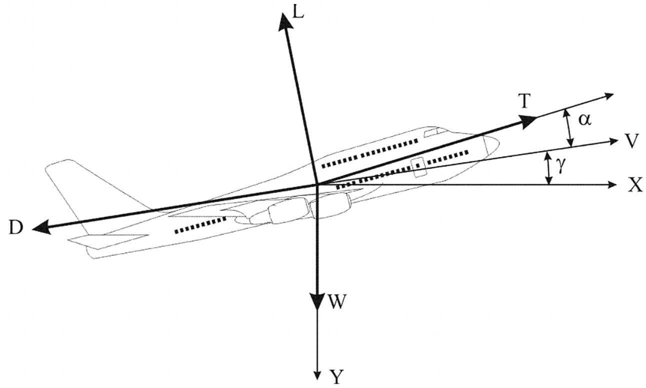

Fig. 2 Two-dimensional model of forces acting on an aircraft.

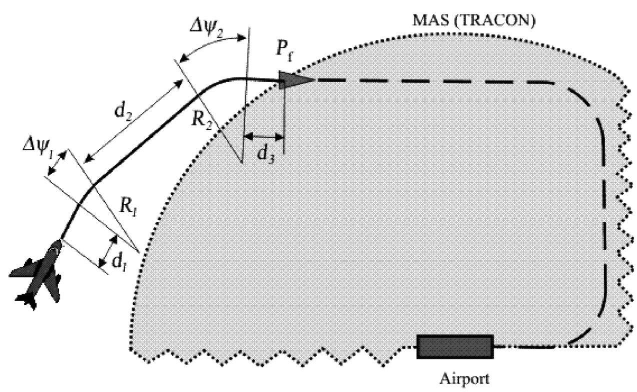

Fig. 3 A five-leg landing trajectory.

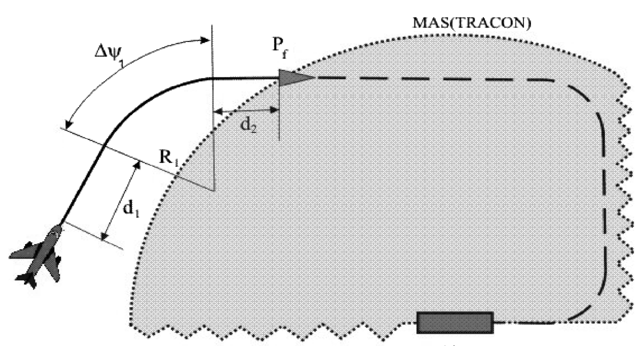

Fig. 4 A three-leg trajectory.

at least proportional to the growth rate of air traffic increases (i.e., 2%). Despite the significant growth in demand, the opportunity to increase the number of airports or even runways is very limited, mainly due to the environmental and geographic constraints. This demands a continuous change in managing air traffic as the most viable near-term solution in relieving airport congestion.

Among different tasks an air traffic controller (ATC) must be trained for, the tasks related to the approach phase are the most critical ones. The simple but powerful method that has been used to schedule aircraft in this phase is based on the so-called *first come, first served* (FCFS) method. The two key advantages of this method are its simple philosophy to implement as well as its sense of fairness [3]. Despite its benefits, the method tends to reduce runway throughput due to its large spacing requirements. This can easily lead to congestions and their associated delays. It also reduces the passengers' sense of safety.

Recently, a number of new concepts have been studied to improve landing management at a controlled airspace. These studies could be divided into two major categories: 1) time scheduling and 2) path planning and conflict detection and resolution (CDR) [4]. Time

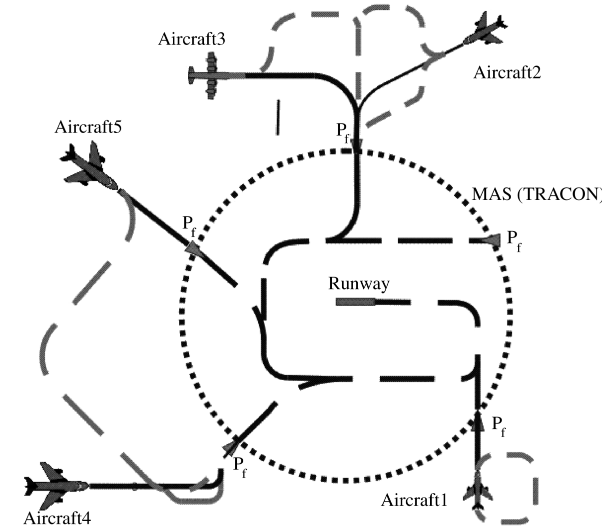

Fig. 5 Some possible Dubin trajectories for approaching aircraft.

scheduling primarily tries to land each aircraft at its expected time of arrival (ETA). In this approach, every aircraft can only land in a specific time window. The time window encompasses minimum landing time as well as its maximum possible value. The latter is determined based on the airplane specifications, performance, and the maximum expected time of arrival based on its available fuel. These parameters normally lead to the subject of time scheduling. On the other hand, studies regarding the time scheduling methods rely on different optimization techniques. For example, [3] uses an approach to handle the problem of time scheduling based on FCFS. The approach uses constrained position shifting for each aircraft as it tries to reach a better solution. [5] uses simulation models to handle the foregoing problem and in [6], some different queue models are examined. Reference [7] uses the Simplex method to solve a more general, and so more complex, problem of landing at multirunway airports. While in a hub-and-spoke model, landing scheduling in spoke airports, which do not usually have considerable management tools, is investigated in [4]. Both [2,8] employ the genetic algorithm (GA) technique to solve the time scheduling problem. These two references are interesting in the sense that GA usually provides a near-optimal solution, the feature of which has been effectively used in this work. Interested readers are encouraged to see [7,9], which provide a complete review of available research on landing management tools and techniques.

It is well noted that scheduling techniques at the best provide the proper sequence to maximize the arrival capacity of an airport. The rest of the work still remains to provide the proper heading and speed to overtake to land the aircraft as close as its ETA. This work, however, concentrates in providing the suitable trajectories while considering the scheduling in a overall scheme.

In almost all current scheduling techniques, ATM software assigns an arrival time to each scheduled aircraft according to the available

Table 1 Parameters of *i*th STARC presented in Fig. 6

Phase			
Straight-line flight		Heading-change flight	
Parameter	Status[a]	Parameter	Status[a]
Initial point $P_{i,0}$	GD/GI	Initial point $P_{i,1}$	GD
Final point $P_{i,1}$	GD	Final point $P_{i,2}$	GD
Direction $\psi_{i,0}$	GD/GI	Initial direction $\psi_{i,0}$	GD
Distance d_i	GI	Final direction $\psi_{i,1}$	GD
——	——	Turn radius R_i	GI
——	——	Turn angle $\Delta\psi_i$	GI
——	——	Turn direction TD_i	GI

[a]GD is a geometrically dependent parameter and GI is a geometrically independent parameter.

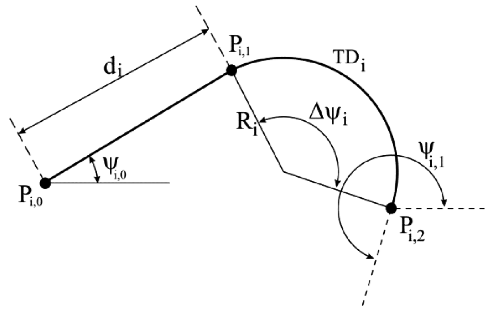

Fig. 6 Maneuver parameters.

time window, known as the assigned time of arrival (ATA). Obviously, as flow of traffic increases, the ATA for any specific aircraft would not necessarily remain the same as its associated ETA. The sum of the squares of the differences between ATA and ETA of n aircraft under consideration forms a function known as *scheduling cost* and could be written as Eq. (1):

$$\mathrm{SC} = \sum_{i=1}^{n} (T_e(i) - T_a(i))^2 \tag{1}$$

where SC is the cost function, n is the total number of aircraft in a specific period of interest, $T_e(i)$ is the expected time of arrival, and $T_a(i)$ is the assigned time of arrival for the ith aircraft.

Nearly all previously mentioned works concentrate on keeping SC of Eq. (1) near a minimum while maintaining an acceptable level of safety in terms of proper separation between any pair of successive aircraft both in distance and time. The key issue here is to combine distance and time in a suitable manner. The time separation is evidently to protect the pursuing aircraft from entering any undesirable aerodynamic vortices caused by the leading one, and its magnitude depends on the type and size of the leader and follower aircraft.

As explained earlier, in addition to minimizing SC of Eq. (1), ATM needs to provide conflict-free trajectories for all approaching aircraft. In this work, we only concentrate on providing conflict-free trajectories for approaching aircraft to land at a controlled aerodrome.

Here, we first examine some recent works to better clarify the contribution of the current work. Reference [10] describes how an optimal path of an aircraft is found such that the pitching moment of the wing-body is minimized. In [11], however, the amount of fuel consumption is monitored as the criterion to find an optimal path, whereas [12] uses GA to only solve for the path planning and tracking part of the problem.

Following NASA's proposal on the so-called free-flight concept as a new approach to ATM problems, much work has been conducted in the field of CDR. For example, [13] uses a hybrid approach to examine different maneuvers to resolve a predicted conflict. In [14], the problem of optimal time control to resolve the conflict is solved using special software referred to as HyTech. This software tool takes advantage of linearization techniques to simplify the problem. There are other references that could be considered as relevant works. For example, [15–18] provide elaborate approaches to resolve a detected conflict during cruising flight. However, they are not applicable to the landing phase, as the flying altitudes are kept constant during the maneuvers.

Table 2 Parameters of trajectory of Fig. 4

Phase			
Straight-line flight		Heading-change flight	
Parameter	Status	Parameter	Status
First STARC parameters			
Initial point $P_{i,0}$	GI	Initial point $P_{i,1}$	GD
Final Point $P_{i,1}$	GD	Final point $P_{i,2}$	GD
Direction $\psi_{i,0}$	GI	Initial direction $\psi_{i,0}$	GI
Distance d_i	GI	Final direction $\psi_{i,1}$	GD
——	——	Turn radius R_i	GI
——	——	Turn angle $\Delta\psi_i$	GI
——	——	Turn direction TD_i	GI
Any interim STARC parameters			
Initial point $P_{i,0}$	GD	Initial point $P_{i,1}$	GD
Final point $P_{i,1}$	GD	Final point $P_{i,2}$	GD
Direction $\psi_{i,0}$	GD	Initial direction $\psi_{i,0}$	GD
Distance d_i	GI	Final direction $\psi_{i,1}$	GD
——	——	Turn radius R_i	GI
——	——	Turn angle $\Delta\psi_i$	GI
——	——	Turn direction TD_i	GI
Final straight-line parameters			
Initial point $P_{i,0}$	GD	——	——
Final point $P_{i,1}$	GD	——	——
Direction $\psi_{i,0}$	GD	——	——
Distance d_i	GI	——	——

Early works regarding air traffic management in the final approach phase were developed in the late 1960s [19]. Careful examination of such works, regardless of some interesting ideas they offer, shows that the resulting controller workload is not justifiable. This phenomenon was mainly due to the technology limitations. Continued growth of air travel through the 1990s led to NASA and Federal Aviation Administration collaboration to develop a new program referred to as the Center TRACON (terminal radar approach control) Automation System (CTAS) [20]. The system is composed of a traffic management advisor, a descent advisor, and a final approach spacing tool (FAST) [21–23].

However, extensive real-time simulations have clearly shown that to produce any appropriate arrival plan, one must consider all possible merges within the terminal airspace and not simply the last merges at the runway threshold [22]. Based on such reasoning, a detailed approach to produce conflict-free trajectories via an en route descent advisor is discussed in [23]. There, the final trajectory patterns come through a trajectory synthesis process. The whole process offers some trajectories based on aircraft dynamics and states, which are good enough to be implemented in real scenarios [23]. Nevertheless, this approach is based on some predefined corridors and would not lead to optimum results.

Our contribution, however, falls in three categories. First, we develop a comprehensive approach to bring an aircraft flying under free-flight rules; that is, we can accept any aircraft entering the controlled aerodrome [for example, less than 10,000 ft above ground level (AGL)]. Second, while keeping the similarity to that of FAST, we consider all issues of time scheduling, path planning, and CDR simultaneously. Third, we add optimality to the whole process.

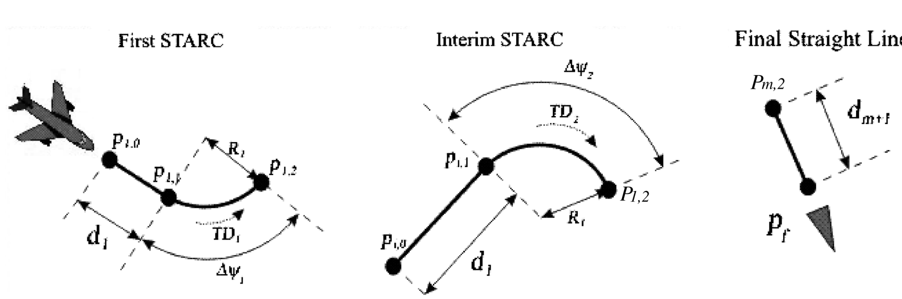

Fig. 7 Parts of a five-leg flight.

Table 3 Parameters list for the last two sets of flight genetic approach

Phase			
Straight-line flight		Heading-change flight	
Parameter	Status	Parameter	Status
$(m-1)$th *STARC parameters*			
Initial point $P_{m-1,0}$	GD/GI	Initial point $P_{m-1,1}$	GD
Final point $P_{m-1,1}$	GD	Final point $P_{m-1,2}$	GD
Direction $\psi_{m-1,0}$	GD/GI	Initial direction $\psi_{m-1,0}$	GD
Distance d_{m-1}	GI	Final direction $\psi_{m-1,1}$	GD
——	——	Turn radius R_{m-1}	GI
——	——	Turn angle $\Delta\psi_{m-1}$	GD
——	——	Turn direction TD_{m-1}	GI
mth *STARC parameters*			
Initial point $P_{m,0}$	GD	Initial point $P_{m,1}$	GD
Final point $P_{m,1}$	GD	Final point $P_{m,2}$	GD
Direction $\psi_{m,0} = \psi_{m-1,1}$	GD	Initial direction $\psi_{m,0}$	GD
Distance d_m	GD	Final direction $\psi_{m,1}$	GD
——	——	Turn radius R_m	GI
——	——	Turn angle $\Delta\psi_m$	GD
——	——	Turn direction TD_m	GI
Final straight-line parameters			
Initial point $P_{m+1,0}$	GD	——	——
Final point P_f	GD	——	——
Direction $\psi_f = \psi_{m,1}$	GD	——	——
Distance d_{m+1}	GI	——	——

In algorithms such as those offered by FAST and its later versions, pFAST and aFAST [22], one would not expect an optimal solution. Fortunately, new and powerful computers are now available that encourage one to develop better algorithms to find improved solutions that are closer to an optimal one. Moreover, the FAST families of algorithms are suited for predefined corridors and are basically not able to respond to needs such as air taxi operations, which demand quick response, or flights under 10,000 ft AGL in general. Different investigations by the authors show that the air taxi operations could not effectively be combined with scheduled flights, as they do not normally use predefined corridors. The math model of this work is its final contribution, which is very straightforward and skips elaborate solution of the full flight dynamics equations. It basically employs both Dubin's theorem [24] and the GA to render a systematic approach to solve an optimization problem without undue complexities.

Dubin's theorem generally states that a trajectory connecting any two points, in the 3-D space, consists of only lines and circular arcs. In the case of flying aircraft, lines might be interpreted as straight-line flights and circular arcs as heading change.

Using a suitable cost function, such as Eq. (1), together with a specialized GA solver, we show how one could compute optimal trajectories in bringing a group of approaching aircraft to a controlled airport. The amount of computation, however, increases enormously, which is not suitable for real-time operation. This shortcoming could simply be overcome by the following:

1) Use more powerful computers or parallel processing.
2) Combine the GA optimization method with a relatively fast decision-making tool, such as fuzzy logic [25].
3) Solve offline for all applicable scenarios and then use a neural network for real-time scenarios.

In this work, we basically employ the first approach to make sure that resulting trajectories satisfy current rules and regulations of a controlled aerodrome, leaving other approaches for later studies.

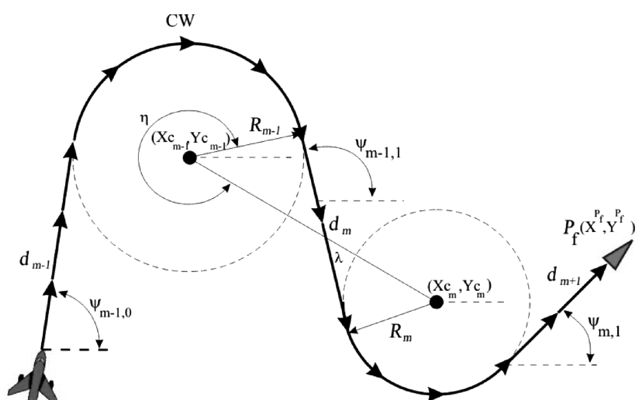

Fig. 8 Graphical presentation of genetic-based approach.

II. Problem Definition

The problem as seen here is to find optimal 4-D trajectories (3-D space plus time) of a known number of aircraft n approaching an airport to land such that a suitable cost function is minimized. The selected cost function considers load factor as an indication of the passenger comfort, fuel consumption, and desired time separation between any two aircraft, satisfying the minimum distances mandated by the appropriate authorities to observe safety. More details about cost function will be presented later. Assuming that approaching aircraft to the designated controlled airport are flying freely (such as an air taxi operation), this work investigates different types of cooperative landing trajectories by proper manipulation of the selected cost function. There are, in fact, no constraints on the initial position, speed, or direction of the approaching aircraft in complying with free-flight concepts.

Use of optimal trajectories during final approach and landing phase of a flight do not normally attract any attention, as these phases are relatively short (although their safety considerations are relatively much higher). Besides, one needs to be certain whether any optimal solution exists before any attempt to find them. This work employs a proven mathematical form based on Dubin's [24] that guarantees existence of a domain of solutions. However, instead of a usual trigonometric approach to find the trajectory, it uses a genetic algorithm as a solver. Based on Dubin, a trajectory connecting any two arbitrary points in a 3-D space consists as a combination of straight lines and circular arcs (Fig. 1). Assuming current aircraft position, together with its final touchdown point on the runway, a mathematical formulation to find a landing trajectory based on Dubin's theorem always contains infinite solutions (not all could be traceable as far as aircraft dynamics is concerned). The remaining task is simply to find the optimum one.

In Fig. 1, if point P_0 refers to the current aircraft position and point P_f refers to the final point, then we look for a suitable set of straight lines and arcs that optimally brings the aircraft at P_0 to the final point P_f. In keeping with the current practice, we consider two separate phases to land any aircraft. We concentrate on the first phase, in which we solve for trajectories that bring the aircraft to the thresholds of a so-called merging airspace (MAS). MAS could be easily selected based on TRACON. The merging direction (ψ_f in Fig. 1) could be any suitable angle based on current traffic. In general, MAS and P_f are selected through consulting with ATM authorities. In the remainder of this manuscript, P_f refers to both a proper merging point together with merging direction. This phase could serve as a transition from the free-flight phase to the second phase, which enjoys structured flight within the controlled airspace.

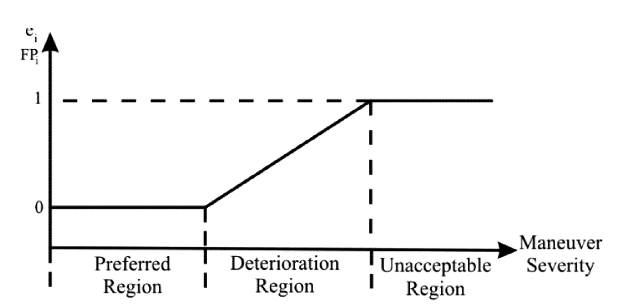

Fig. 9 A general bilinear model introducing preferred and allowable limits.

Table 4 Properties of airplane classes

Class	Price, \$	a_{max}, g	a_{mid}, g	φ_{max}, deg	φ_{mid}, deg	SFC, L/h
Heavy	200 million	0.2	0.02	40	25	5000
Medium	80 million	0.2	0.05	50	30	2000
Light	30 million	1	0.5	70	40	1000

Table 5 Typical maximum and minimum number of genes N and resolution δ of parameters used for GA

Parameter	Symbol	Min.	Max.	N	δ
$(m-1)$th turn radius	R_{m-1} m	0	100,000	8	391
mth turn radius	R_m m	0	100,000	8	391
$(m-1)$th and mth turn directions	TD_{m-1}, TD_m	1	4	2	1
$(m-1)$th distance	d_{m-1} m	100	200,000	8	781
$(m+1)$th distance	d_{m+1} m	100	200,000	8	781

In the second phase, the aircraft usually follows directions given by the control tower. Although the current approach is very much applicable to the second phase, we mostly concentrate on the first phase of the flight.

As can be seen, this approach, while respecting the current practice, provides an optimal trajectory to land any aircraft. The mathematical algorithm is not sensitive to the initial position of the aircraft (P_0), therefore, it also enjoys the benefit of a free approach up to the controlled airspace (P_f). Here, we also respect Federal Aviation Regulation Part 91 [26], which defines altitude and speed restrictions at and around airports in the U.S. airspaces. Such typical restrictions could be used as the trajectory constraints during computation process. Although, it is worth noting that satisfying all constraints would increase the computation time and so limits the possibility of real-time applications.

A. Aircraft Equations of Motion

Consider an aircraft as a point mass moving in 2-D space, with fixed configuration and no thrust vectoring. Using the terms defined in Fig. 2, and assuming a flat Earth and no wind condition, the necessary equations of motion are as follows:

$$\dot{y} = -\nu \sin\gamma \tag{2}$$

$$\dot{x} = \nu \cos\gamma \tag{3}$$

$$\dot{\nu} = (T\cos\alpha - D)/m - g_o \sin\gamma \tag{4}$$

$$\dot{\gamma} = (T\sin\alpha + L)/m\nu - g_o \cos\gamma/\nu \tag{5}$$

$$L = qsC_L, \qquad D = qsC_D \tag{6}$$

The aircraft thrust force could be expressed as a nonlinear function of engine size and power $g(\eta)$, which should be available to the trajectory designer:

$$T = T_{\max}(M, y)g(\eta) \tag{7}$$

Equations (2–7) present a complete set of equations of motion in a vertical plane. A similar approach could be used to model turning flights in a horizontal plane. The aircraft mathematical model as presented here is a highly nonlinear one and would take a considerable amount of time and effort to find an optimal trajectory that brings an aircraft from given point A to a destination B. Instead of going through an elaborate solution, in this work, we use an elegant simplification based on Dubin's theorem together with the use of GA, described in the following subsection. For simplicity, we refer to the resulting solutions as *genetic optimal Dubin trajectories*, or simply GODT.

B. Dubin Trajectory Patterns

With an arbitrary P_0, a typical Dubin trajectory is as shown in Fig. 1, noting that the en route part of the flight is of no importance in the mathematical model. One observes that any trajectory connecting P_0 to P_f consists of different segments, and each segment contains

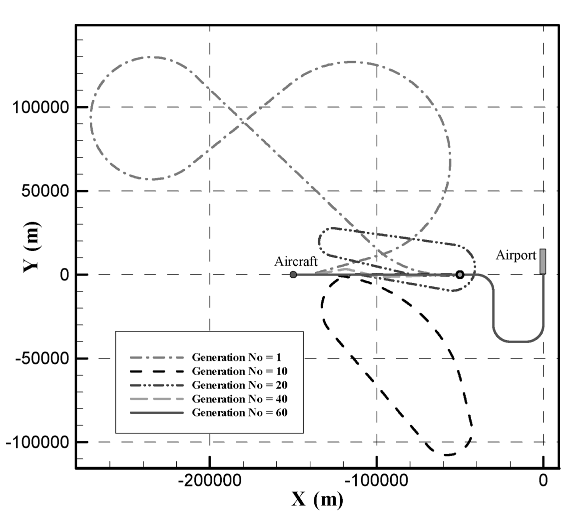

Fig. 10 Best trajectories during different generations.

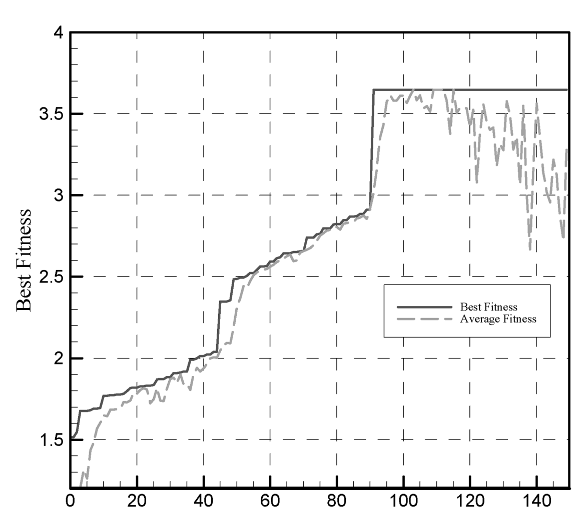

Fig. 11 Best fitness and average fitness variation with generations.

Table 6 Properties of the aircraft for comparison of trajectories for different types of aircraft

Aircraft no.	Type	Mass, t	Initial velocity, m/s	Initial height, km	Final velocity, m/s	$X0$, km	$Y0$, km	Initial direction	N_A to P_f	X of P_f, km	Y of P_f, km	Direction at P_f	N_A after P_f
1	——	——	260	12	100	−90	30	0	3	−50	30	335	3

a straight line followed by an arc, referred to as STARC in this work. An arc is simply an indication of a change in the aircraft heading angle. As an example, the aircraft shown in Fig. 3 follows a trajectory that consists of two heading changes and three straight lines (a five-leg trajectory with two STARCs), and the one in Fig. 4 follows a trajectory consisting of only one heading change and two straight lines (a three-leg trajectory with one STARCs). Both trajectories, however, are completed with some predefined-structured trajectory, which starts at P_f and ends at the runway touchdown area in the TRACON or MAS. The optimization process here searches for the best possible number of STARCs, thus providing the GODT, similar to that of Figs. 3 and 4. There is no limitation in the number of segments (STARCs) in a trajectory; however, different case studies conducted by the authors show that trajectories with maximum three legs (2-STARC) provide enough flexibilities while dealing with just one aircraft. As the number of aircraft increases, more elaborate patterns with more STARCs are needed (Fig. 5).

The contribution of this work falls in different categories. First, we lower the level of mathematical complexities by using predefined Dubin trajectories while computing optimal trajectories. Second, we use GA as a powerful heuristic search method together with a comprehensive cost function that can handle different management point of views. We have kept the approach fast enough for real-time applications while involving one or two aircraft approaching a controlled aerodrome. Third, our GODT plays as an interface between the en route part of flight and the part associated with TRACON, thus easily implementable without interfering with current infrastructure. Fourth, in our approach the equations of motion are not directly solved to find the trajectories; instead, they are used as some constraints that are considered in the cost function.

In Fig. 5, P_f denotes the point at which MAS starts and an aircraft follows a structured path as directed by the controlling authorities (ATC). Changing P_f provides different optimal patterns for the resulting trajectory and so brings insight to the ATC, and so it is a good practice to even select it at the runway touchdown point.

The optimal solution, as referred to in this work, leads to some parameters that define the GODT for all (or selected) approaching aircraft. For further clarity, the parameters defining a STARC trajectory are given in Table 1 and Fig. 6. The table also shows the nature of each parameter as being either geometrically dependent or geometrically independent. A geometrically independent parameter

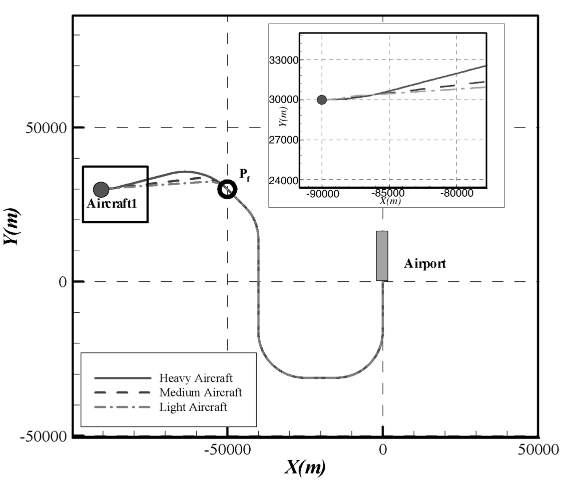

Fig. 12 Comparison of optimal trajectory for different types of aircraft (case 1).

denotes those that are selected by the optimizer, and a geometrically dependent parameter is calculated using geometrical constraints. For more complex trajectories, a typical approach could easily be adopted to suit the user's need. That is, a STARC could be repeated as many times as needed (Fig. 7). Again, case studies show that the nature of the geometrically dependent and geometrically independent parameters might be changed as the number of STARCs change (Table 2).

A Dubin trajectory ignores the fact that we are dealing with an aircraft, as it sees the aircraft as just a flying point. Proper examination of different Dubin trajectories to land an aircraft shows that following the last STARC, the aircraft must have a proper heading angle as dictated by the ATC. This imposes a severe constraint that must properly be investigated, as it forces only a portion of the solution space to be acceptable. This becomes very cumbersome when an optimum solution is located on a tiny domain of possible solutions that could be missed very easily. In such cases we need to make sure that all possible domains of solutions enjoy the same chance during the optimization process.

To do so, a new parameter, STR, is introduced that shows the sequence of turn directions for all the turns in a trajectory pattern. For example, if there are two turns in a trajectory, then the aircraft could use any of four possible sets of

$$\{(\mathrm{CW}, \mathrm{CW})(\mathrm{CW}, \mathrm{CCW})(\mathrm{CCW}, \mathrm{CW})(\mathrm{CCW}, \mathrm{CCW})\}$$

as STR. In fact, STR helps to properly select the most appropriate solution while dealing with population-based optimization techniques.

Different case studies conducted by the authors show that the following set of parameters, together with all independent maneuvers parameters before the $(m-1)$th turn, works relatively well:

$$\{(\mathrm{STR})(d_{m-1})(d_{m+1})(R_{m-1})(R_{m+1})\}$$

A complete list of parameters is presented in Table 3. Equations (8–16) define the geometrical relationships for Fig. 8, which is for STR selected to be (CW, CCW). One could use a similar approach to formulate other possible strategies:

$$X_{m-1,1} = X_{m-1,0} + d_{m-1}\cos(\psi_{m-1,0}) \tag{8}$$

$$\begin{aligned} Xc_{m-1} &= X_{m-1,1} - R_{m-1}\cos(\psi_{m-1,0}) \\ Yc_{m-1} &= Y_{m-1,1} + R_{m-1}\sin(\psi_{m-1,0}) \end{aligned} \tag{9}$$

$$Xc_m = X^{P_f} - d_{m+1}\cos(\psi_{m-1,1}) - R_m\sin(\psi_{m-1,1}) \tag{10}$$

$$\eta = \tan^{-1}((Yc_m - Yc_{m-1})/(Xc_m - Xc_{m-1})) \tag{11}$$

$$\lambda = \sin^{-1}((R_{m-1} + R_m)/\sqrt{(Xc_m - Xc_{m-1})^2 + (Yc_m - Yc_{m-1})^2} \tag{12}$$

$$\psi_{m-1,1} = \eta - \lambda \tag{13}$$

$$\Delta\psi_{m-1} = \psi_{m-1,1} - \psi_{m-1,0} \tag{14}$$

Table 7 Parameters of optimal trajectories of Fig. 12 (case 1)

	STARC no. 1			STARC no. 2			STARC no. 3						
Type	D, m	R, m	Θ, deg	D, m	R, m	Θ, deg	D, m	R, m	Θ, deg	Last straight length, m	Time, s	Distance, m	Cost of consumed fuel
H	0	19,216	14.2	0	19,216	0.5	17,197	19,216	59.7	28	917.9	165,223	12,749
M	0	12,157	5.7	0	12,157	1	28,719	12,157	51.8	29	912.2	164,206	5,068
L	0	8,235	1.5	0	8,235	2.6	33,045	8,235	49.1	42	909.9	163,778	2,527

Table 8 Properties of two aircraft with a conflict in their individual optimal trajectory (case 3)

Aircraft no.	Type	Mass, t	Initial velocity, m/s	Initial height, km	Final velocity, m/s	$X0$, km	$Y0$, km	Initial direction, deg	N_A to P_f	X of P_f, km	Y of P_f, km	Direction at P_f, deg	N_A after P_f
1	L	6	180	0.5	100	−80	45	0	3	−30	20	0	3
2	L	6	180	0.5	100	−80	−5	0	3	−30	20	0	3

$$D_2 = (R_{m-1} + R_m)/\tan(\gamma) \tag{15}$$

$$\Delta\psi_{m,1} = \psi_{m,1} - \psi_{m-1,1} \tag{16}$$

C. Cost Function Formulation

It is well known that the merit of any optimum solution is highly related to the merit of its associated cost function that manages the search toward the final solution. In this work, we use a systematic approach to bring all contributing factors into the cost function. This increases the mathematical complexities but provides a clear vision for a potential user to better understand the contribution of each factor in the final solution. The contributions are as follows:

1) The cost of maintaining a spatial separation minima between any two adjacent aircraft, is shown by $\mathrm{Cost}|_{\delta x}$.

2) The cost associated with flight time and fuel cost is shown by $\mathrm{Cost}|_{\mathrm{Time}}$.

3) The cost associated with flying quality such as passenger satisfaction is shown by $\mathrm{Cost}|_{\mathrm{FQ}}$.

4) The cost associated with keeping a time separation between any two successive aircraft is $\mathrm{Cost}|_{\delta t_{i,j}}$.

The total cost, then, is given in Eq. (17):

$$\mathrm{Cost} = \mathrm{Cost}|_{\delta X} + \mathrm{Cost}|_{\mathrm{Time}} + \mathrm{Cost}|_{\mathrm{FQ}} + \mathrm{Cost}|_{\delta t} \tag{17}$$

Assuming $\mathrm{Cost}|_{\delta x}(i,j)$ as the cost of having a conflict between two aircraft i and j, then the total cost $\mathrm{Cost}|_{\delta x}$ could be expressed as

$$\mathrm{Cost}|_{\delta x} = \frac{1}{2}\sum_{i=1}^{n}\left(\sum_{j=1, j\neq i}^{n}\mathrm{Cost}|_{\delta x}(i,j)\right) \tag{18}$$

where $\mathrm{Cost}|_{\delta x}(i,j) = \mathrm{Cost}|_{\delta x}(j,i)$.

To explain how cost introduced by Eq. (18) affects the optimal solution, we need to use a new factor, as violating a separation minimum would not necessarily lead to an accident. Equation (19), in fact, uses a probability factor given by $P(\delta X|_{i,j})$ based on the current value of each aircraft ($L|_{\mathrm{Aircraft}}$) to account for the risk of accident in case of violating the separation minima. A normal distribution is further assumed for $P(\delta X|_{i,j})$ as described in Eq. (20):

$$\mathrm{Cost}|_{\delta X}(i,j) = P(\delta X|_{i,j})(L|_{\mathrm{Airplane}_i} + L|_{\mathrm{Airplane}_j}) \tag{19}$$

$$P(\delta X|_{i,j}) = e^{-(\zeta\delta X|_{i,j})_2} \tag{20}$$

where δX is the minimum distance between any two aircraft i and j during their flight, and ζ is used to vary the radius of conflict. In case studies we select ζ such that $P(\delta X|_{i,j}) = 0.1$ at $\delta X = 5$ nm.

Assuming any aircraft linearly decelerates throughout the approach phase, the cost associated with the flight time and energy would then be as given by Eq. (21). One might note that the second term in Eq. (17) is the same as the cost of consumed fuel:

$$\mathrm{Cost}|_{\mathrm{Time}} = L_f\sum_{i=1}^{n} c_i t_i \tag{21}$$

where C_i represents the specific fuel consumption of aircraft i, L_f is the current fuel price, and t_i represents the flight time and could easily be approximated using average velocity of the aircraft.

For the cost associated with the ride quality, we use Eq. (22). With Eq. (22), we are considering a cost that accounts for the passenger satisfaction with three distinctive levels given by FP_i. The passenger satisfaction deteriorates as the severity of maneuvers during the trajectory increases. In general, passengers prefer more straight-line flights or turns with minimal load factor, which are not always possible:

$$\mathrm{Cost}|_{\mathrm{FQ}} = \sum_{i=1}^{n}(FP_i(\mathrm{man})L|_{\mathrm{Airplane}_i} + k_i N_i e_i(\mathrm{man})L|_{\mathrm{Airplane}_i}) \tag{22}$$

Both e_i and FP_i follow a general bilinear model that describes three regions (Fig. 9). The first region shows the acceptable area, the third region designates the unacceptable one, and the region in between shows a transition from acceptable to unacceptable. Here, we assume that the transition occurs linearly, between the two user-selected bounds.

In Eq. (22), N_i shows the number of passengers in the ith aircraft, and k_i represents the priority of aircraft i. Here, we relate passenger satisfaction during a heading change e_i(turn) to the bank angle imposed onto the aircraft. Having an idea regarding the bank angle limits (φ_{mid} or φ_{max}), we might calculate its associated cost. On the

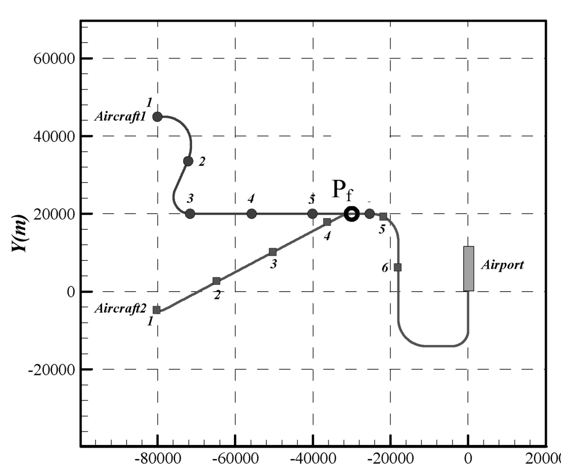

Fig. 13 Optimal landing trajectories of two aircraft regarding CDR (case 3).

Table 9 Parameters of optimal trajectory of Fig. 13 (case 3)

	STARC no. 1			STARC no. 2			STARC no. 3					
AC no.	D, m	R, m	Θ, deg	D, m	R, m	Θ, deg	D, m	R, m	Θ, deg	Time, s	Distance, m	Cost of consumed fuel
1	0	19,607	8.6	8,235	32,156	3.4	130,917	43,137	12.0	1,147	263,836	15,932
2	21,569	21,176	65	9,804	21,176	107	79,212	19,216	42	1,300	298,934	18,052

Table 10 Properties of two aircraft with considerable difference in velocity (case 4)

Aircraft no.	Type	Mass, t	Initial velocity, m/s	Initial height, km	Final velocity, m/s	$X0$, km	$Y0$, km	Initial direction, deg	N_A to P_f	X of P_f, km	Y of P_f, km	Direction at P_f, deg	N_A after P_f
1	L	10	500	12	120	−300	40	0	3	−60	40	0	3
2	H	200	200	12	70	−250	40	0	3	−60	40	0	3

other hand, in a straight-line flight, rate of descent (a_{mid} and $a_{\max}$) plays the same role. In this work, we use the same level of importance for e_i and FP_i. Other terms are introduced in the Nomenclature.

The last element in the cost function relates to the cost incurred due to imposing proper time separation between any two successive aircraft. We estimate such cost using Eq. (23):

$$\mathrm{Cost}|_{\delta t_{i,j}} = FP_i(\delta t_{i,j-1})L|_{\mathrm{Airplane}_i} \tag{23}$$

where $FP_i(\delta t_{i,j-1})$ shows the probability of the ith aircraft to abort landing due to the wake vortex of the previously landed aircraft. Reference [3] provides the necessary information that helps calculate such a term for the case studies presented in this work. Here, we recognize three different classes of aircraft: HL (heavy with low maneuverability), MM (medium with low-to-medium maneuverability), and LH (light with high maneuverability). For each category, all parameters such as φ_{mid}, $\varphi_{\max}$, a_{mid}, and $a_{\max}$ are precisely selected; typical values are as given in Table 4.

III. Optimization Technique and Verification

The nature of optimization problem here falls into the category referred to as multi-island optimization problems. In reality, the number of islands depends on the number of aircraft and so the complexity of the optimization problem grows with the number of aircraft together with the number of parameters to be optimized for each island. Gradient-based optimization techniques usually fail to solve a problem of this size. Stochastic optimization methods, on the other hand, can find the global minimum more efficiently. In this work, two different techniques of simulated annealing [27] as well as GA [28] were used to enhance the degree of assurance in reaching an optimal solution; however, we only present the GA results, as they proved to be more practical.

GA is a well-known stochastic optimization method that is currently used in many fields. The basic concept of GA was presented in 1960 by Holland [29]. The method encodes any potential solution to the optimization problem into chromosomelike structures and allows them to compete, reproduce, and mutate to create better solutions over generations. In this work, two other operands, called creep and elitism, are also employed to enhance the quality of the results.

The authors used an in-house improved version of an available GA code, called IMPROVE. Other codes are also available that might be modified to match the requirements for landing management problems. It is noted that GA parameters such as population number, mutation frequency, and crossover probability differ for different problems. This might lead to quite a few numbers of trials to select the proper resolution to search the solution space. In this work, depending on the number of aircraft and their relative distance from the destination airport, the minimum, maximum, number of genes, and resolution for each optimization parameter are presented in Table 5.

To verify the validity of the developed optimization approach, a simple case was investigated. The case involves just one aircraft flying from P_0 to P_f without any constraint. It is clear that the solution must be a simple straight line. We would like to see whether Dubin and GA would provide such a solution. To make it even harder, we use a 4-STARC Dubin trajectory. The best of the obtained optimal trajectories in different generations are presented in Fig. 10, with their associated average fitness variation in Fig. 11. It is clear that the developed algorithm finally finds the proper solution, which is a straight line connecting P_0 to P_f.

IV. Case Studies and Results

An efficient graphical user interface (GUI) in the C# language together with IMPROVE were employed for the case studies, some results of which are presented here. The GUI accepts the aircraft parameters and initial position P_0 in addition to the desired P_f and uses the IMPROVE code to find the optimum trajectories. The GUI also shows the real-time update of the trajectories over the generations during the evolution.

Here, we start from cases involving only one aircraft looking at different preferences for landing. Then we increase the number of aircraft and compare to the previous cases. We limit ourselves to a case involving three aircraft, for it is quite difficult to demonstrate the resulting trajectories for the case of four aircraft and more.

A. Cases Involving One Aircraft

When dealing with one aircraft, as there is no other aircraft involved, it would be desirable to follow trajectories that minimize the fuel consumption while maneuvers remain as comfortable as possible. Table 6 shows the initial conditions of each aircraft

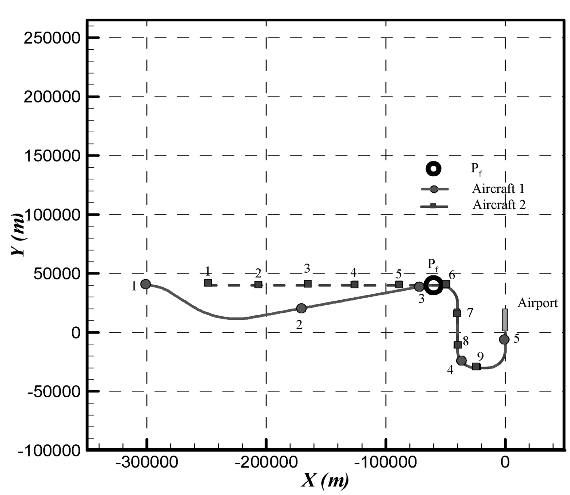

Fig. 14 Optimal safe overtaking in a case with considerable difference in velocity (case 4).

Table 11 Parameters of optimal trajectory of Fig. 14 (case 4)

	STARC no. 1			STARC no. 2			STARC no. 3						
AC no.	D, m	R, m	Θ, deg	D, m	R, m	Θ, deg	D, m	R, m	Θ, deg	Last straight length, m	Time, s	Distance, m	Cost of consumed fuel
1	0	35,294	32.6	21,961	70,196	43.1	144,426	52,157	10.5	344	1,257.6	389,862	3,493
2	32,157	8,627	0.1	0	11,372	0.1	124,867	22,745	0	32,976	3,006.2	330,686	41,753

Table 12 Properties of three aircraft with a conflict in their individual optimal trajectory (case 5)

Aircraft no.	Type	Mass, t	Initial velocity, m/s	Initial height, km	Final velocity, m/s	$X0$, km	$Y0$, km	Initial direction, deg	N_A to P_f	X of P_f, km	Y of P_f, km	Direction at P_f, deg	N_A after P_f
1	H	100	260	12	80	−200	80	0	3	−80	50	315	3
2	L	10	380	12	100	20	130	180	3	−80	50	315	3
3	H	100	260	12	80	−150	−100	60	3	−40	−48	0	1

regardless of its type. Here, N_A refers to the number of possible STARCs (Table 1) both between P_0 and P_f and between P_f and the touchdown point.

Figure 12 and Table 7 show the optimum trajectories. It is clear that the aircraft type influences its optimum landing trajectory in that an aircraft with relatively less maneuvering capabilities (solid line) uses a lengthier trajectory to land. It is also interesting to note that we see only three legs (2-STARC) from P_0 to P_f, which is less than what was originally allowed. That is, the optimization process automatically reduces the number of legs to a minimum.

Comparing the results shows that there are no meaningful differences in the resulting trajectories as far as the aircraft type is concerned. A careful study of the equations reveals that the turn radius depends directly on the aircraft type. In fact, turn radius is a function of maximum bank angle, which is highly dependent on the size of the aircraft. It also depends on the aircraft velocity, the effects of which are negligible in this case.

B. Cases Involving Two Aircraft

Previous cases involving one aircraft shows that optimal trajectories are such that the aircraft changes its heading quickly toward the P_f and then follows a straight line toward it and finally adjusts its heading for the final merge. This pattern is also valid for cases involving multiple aircraft if their respecting trajectories are not in conflict. If there is a conflict in the resulting trajectories, then the developed method needs to resolve the conflict and find new trajectories as the cost function dictates. We investigate two cases with the initial conditions of Table 8.

Figure 13 together with Table 9 show the results for two similar aircraft attempting to land at the same destination. The figure also shows the position of either aircraft in scaled time steps to help locate their relative distance. It is clear that the developed algorithm assigns a relatively lengthier trajectory to one of the aircraft to postpone its arrival at the destination. Obviously, such a solution is not unique and we could simply get different trajectories by changing, for example, the passenger comfort for one of the two aircraft.

Cases involving two aircraft become more interesting as soon as one of the two attempts to overtake the other. The current method could effectively propose safe overtaking trajectories, as shown in case 4. Table 10 provides the necessary data for two aircraft that are again attempting to land at the same destination, and we seek for trajectories that allow no. 1 to overtake no. 2. The resulting trajectories are shown in Fig. 14 and Table 11.

When overtaking is not an option, aircraft no. 1 lands at 3202 s (calculation not shown here) and no. 2 lands at 3006 s. However, Table 11 shows that by overtaking, we are able to land no. 1 at 1257 s, which provides 1944 s savings in flight time in cases of emergencies, without interfering with no. 2 trajectory.

C. Cases Involving Three Aircraft

In case 5, we investigate three aircraft approaching a common destination. The initial conditions of all aircraft are given in Table 12 and are such that if all aircraft follow their individual optimal trajectories, the sequence of landing is 3-2-1 (Fig. 15). However, such trajectories are clearly in conflict for nos. 1 and 2 (Fig. 15). We now seek for trajectories that are conflict-free. As seen, no. 2 is a light airplane, so we expect the algorithm to give a lower priority to it as opposed to no. 1. The resulting trajectories are shown in Fig. 16. In the new sequence (3-1-2), the total fuel consumption is minimized

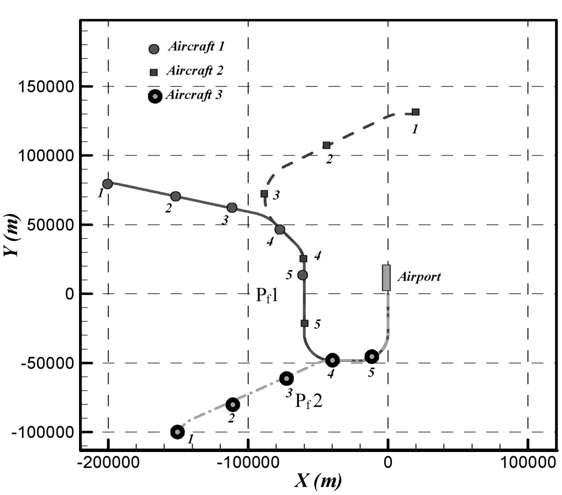

Fig. 15 Optimal trajectories in case of three aircraft (case 5) without considering the conflict.

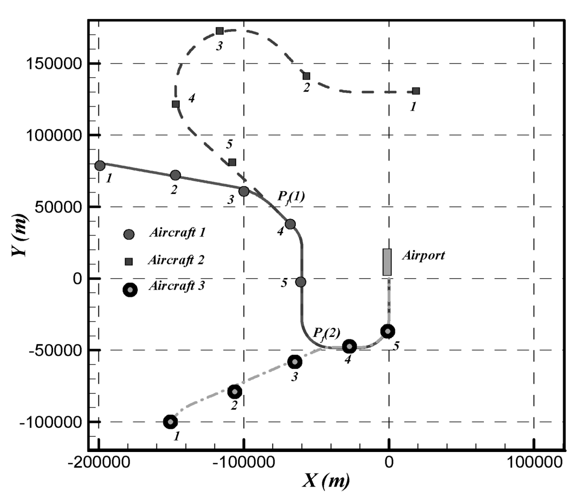

Fig. 16 Optimal conflict-free trajectories in case of three aircraft (case 5).

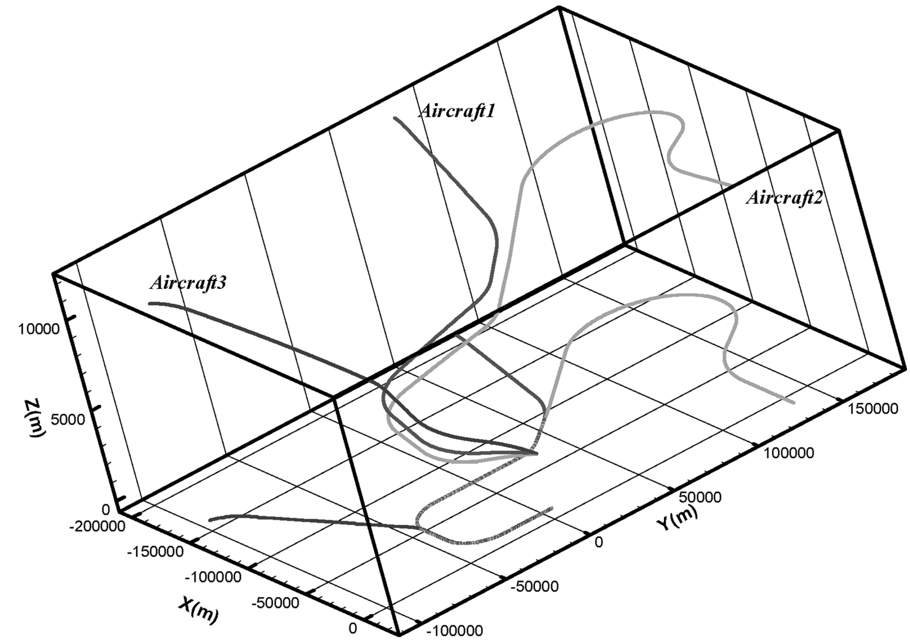

Fig. 17 Three-dimensional presentation of optimal trajectories of aircraft (case 5).

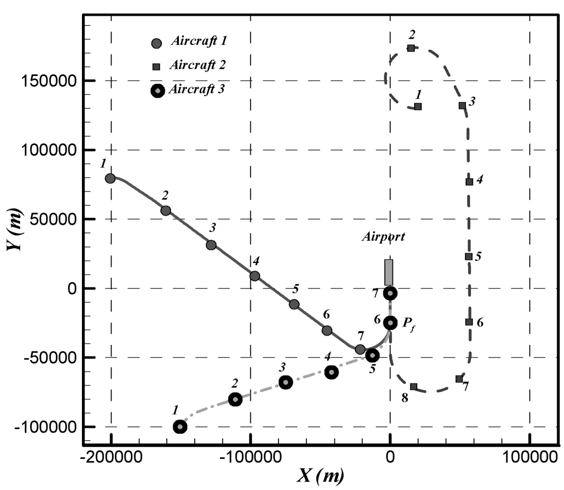

Fig. 18 Optimal conflict-free trajectories in the case of three aircraft (case 6).

while maintaining conflict-free trajectories with proper time separations toward the destination airport. Again, as GA provides near-optimal trajectories; the solution would not be unique and by simply changing the terms in the cost function we might get other solutions. This of course, gives flexibility to a controller to try different options when time allows.

Figure 17 shows the 3-D representation of all three trajectories, for which the final point is 3000 (m) AGL. That is, the optimization process ends there. In fact, this is the point at which ATC forces the aircraft to follow predefined paths, not those suggested by the optimal solution. To show how this might be used, we study the effect of changing Pf in case 5. Case 6 shows what happens if we force all three aircraft to use the same Pf. Figure 18 shows the results. Comparing Figs. 17 and 18 shows how no. 2 is forced to make a tight turn and approach the airport from the opposite side that it used in Fig. 17. Table 13 compares the other aspects of the two cases. One might also notice that, overall, case 6 exhibits a better performance, as it helps land all three aircraft in 11% shorter time.

Table 13 Comparison of a three-aircraft landing scenario with two different merge points (cases 5 and 6)

	Case 5			Case 6		
Aircraft no.	Time	Distance	Cost	Time	Distance	Cost
1	1,895	322,131	26,327	1,624	276,059	22,554
2	2,126	510,282	5,915	1,836	440,701	5,101
3	1,191	202,520	16,546	1,180	200,627	16,391
Total	5,212	——	48,788	4,640	——	44,046

D. Effect of Wind on Optimal Trajectories

Trajectories presented so far do not consider the wind effects while approaching a typical runway, although this is an important issue, especially for light aircraft with low stall speeds. Moreover, from a practical point of view, we need to examine the so-called robustness of the GA-resulting trajectories. That is, one is always interested to see how small changes (or even errors) in declaring the aircraft initial position as well as flight speed would affect the optimal trajectories. Such cases clearly happen when we are dealing with a windy atmosphere. So it is important to see how wind speed would affect the optimal trajectories provided by the current solver. Some recent works have studied the effect of wind on Dubin's trajectories with enough rigor in mathematics: for example, [30] uses general optimal theory to conduct such studies. In this work, however, we find it more appropriate to incorporate the effect of wind into the cost function itself. This approach, although approximate, suits the nature of numerical optimization based on GA. Different case studies conducted by the authors show that for the case of single aircraft, the effect of wind in the form of a tailwind (or headwind) could simply be added to or subtracted from the aircraft speed and has no dramatic

Table 14 Effect of wind on the optimal trajectories and sequence of landing (cases 7–9)

Aircraft no.	v, m/s	v_w, m/s	Time of flight, s
		Case 7	
1	160	0	2,006.2
1	160	10 tail	1,935.0
1	160	10 head	2,085.7
		Case 8	
1	160	0	2,164
2	160	0	1,943
		Case 9	
1	160	10 tail	1,988
2	160	10 head	2,262

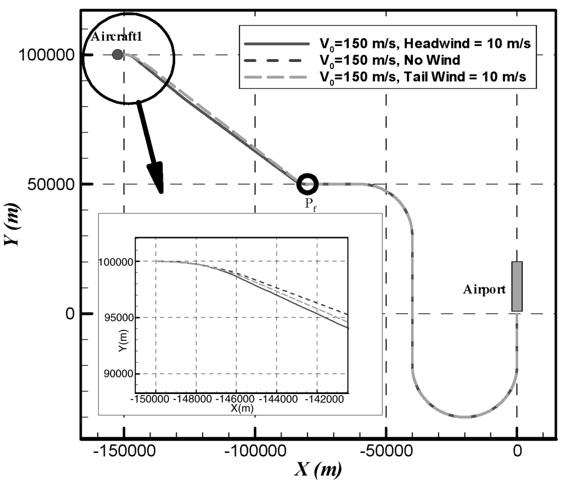

Fig. 19 Effect of wind direction on the optimal trajectories (case 7).

effect on the resulting trajectories. It is well noted that we prefer to have a quick but near-optimal solution. However, in the case of two or more aircraft, depending on the aircraft initial positions, some aircraft see the wind as a tailwind and some see that as a headwind, so the resulting trajectories would dramatically change. Case nos. 7, 8, and 9 clearly show the affect of wind on the optimal trajectories (Figs. 19 and 20 and Table 14). In these cases, not only are the trajectories different, but the sequence in which the aircraft are allowed to land also changes, due to a wind speed even less than 10% of the aircraft initial speed. This simple example shows the importance of this work and why a quick (real-time) but near-optimal solution is in fact more practical than a precise offline solution.

V. Conclusions

The current work aims to be an advocate of the so-called free flight, especially for small or very light aircraft operating in and out of class C or D airports. The approach also seems to be to the benefit of the so-called small air transportation system. It also helps demonstrate the ability of the GA method in difficult optimization problems, such as conflict-free trajectories during approach. With fast and powerful computers, it could also serve as an effective landing management tool. Even an offline application of the method could bring very good insight for any controller and might easily be used as a training tool. For real-time application, however, further research might be necessary to allow solving for different options, such as changing Pf as discussed in case 6. We also need a proper way to pass the results to all pilots involved. The authors believe that emerging technologies in the area of mobile phones, such as medium-size messaging system that could transfer pictures, could be used to transfer the resulting trajectories to the pilots involved. Devices such as tactical collision avoidance system could also be modified to accept graphical solutions transmitted by a powerful computer located at the airport during the approach phase of the flight.

To bring more speed to the calculation process, one might conduct extensive offline studies for all desired approach and landing scenarios together with possible wind speed and directions and then effectively employ a neural network to rapidly propose proper trajectories. Nevertheless, based on the in-house investigations, the authors believe that more computing power through parallel processing is more efficient when dealing with windy conditions. Obviously, actual flight-test studies would also be required to finalize these findings.

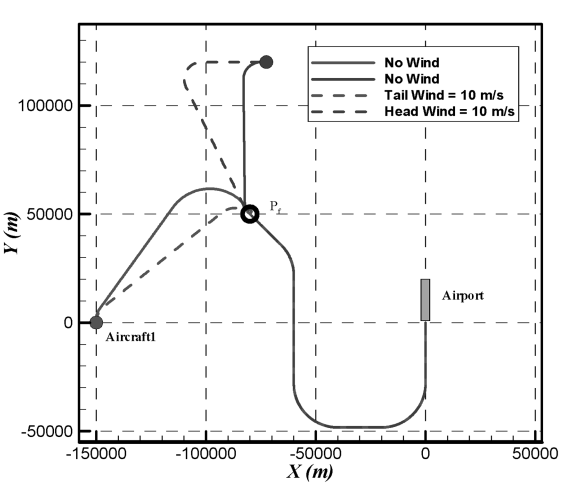

Fig. 20 Effect of wind on the sequence of landing (cases 8 and 9).

References

[1] "FAA Aerospace Forecasts Fiscal Years 2007–2020," Federal Aviation Administration, Feb. 2009.
[2] Ciesielski, V., and Scerri, P., "Real Time Genetic Scheduling of Aircraft Landing Times," *Proceedings of the IEEE International Conference on Evolutionary Computation (ICEC98)*, Inst. of Electrical and Electronics Engineers, Piscataway, NJ, 1998, pp. 360–364.
[3] Balakrishnan, H., and Chandran, B., "Scheduling Aircraft Landings Under Constrained Position Shifting," AIAA Guidance, Navigation, and Control Conference and Exhibit, Keystone, CO, AIAA Paper 2006-6320, 2006.
[4] Ding, Y., Rong, J., and Valasek, I., "Feasibility Analysis of Aircraft Landing Scheduling for Non-Controlled Airports," AIAA Guidance, Navigation, and Control Conference and Exhibit, AIAA Paper 2004-5241, 16–19 Aug. 2004.
[5] Andreussi, A., Bianco, L., and Riccardelli S., "A Simulation Model for Aircraft Sequencing in the Terminal Area," *European Journal of Operational Research*, Vol. 8, No. 4, Dec. 1981, pp. 345–354.
[6] Milan, J., "The Flow Management Problem in Air Traffic Control: A Model of Assigning Priorities for Landings at a Congested Airport," *Transportation Planning and Technology*, Vol. 20, No. 2, 1997, pp. 131–162.
doi:10.1080/03081069708717585
[7] Ernst, A. T., and Krishnamoorthy, M., and Strorer R. H., "Heuristic and Exact Algorithms for Scheduling Aircraft Landings," *Networks*, Vol. 34, No. 3, 1999, pp. 229–241.
doi:10.1002/(SICI)1097-0037(199910)34:3<229::AID-NET8>3.0.CO;2-W
[8] Hansen, J. V., "Genetic Search Methods in Air Traffic Control," *Computers and Operations Research*, Vol. 31, No. 3, 2004, pp. 445–459.
doi:10.1016/S0305-0548(02)00228-9
[9] Beasley, J. E., Krishnamoorthy, M., Sharaiha, Y. M., and Abramon, D., "Scheduling Aircraft Landings—The Static Case," *Transportation Science*, Vol. 34, May 2000, pp. 180–197.
doi:10.1287/trsc.34.2.180.12302
[10] Trent, A., Venkataraman, R., and Doman, D., "Trajectory Generation Using a Modified simple shooting Method," *Proceedings of the IEEE Aerospace Conference*, Vol. 4, Inst. of Electrical and Electronics Engineers, Piscataway, NJ, 2004, pp. 2723–2729.
[11] Slattery, R., "Fuel-Conservative Four Dimensional Arrival Trajectories Using Terminal-Area Constraints," *AIAA Guidance, Navigation, and Control Conference and Exhibit*, San Diego, CA, AIAA Paper 1996-3874, 29–31 July 1996.
[12] Kanury, S., and Song, Y. D., "Flight Management of Multiple Aerial Vehicles Using Genetic Algorithms," *Proceedings of the 38th Southeastern Symposium on System Theory*, Vol. 5, No. 7, Inst. of Electrical and Electronics Engineers, Piscataway, NJ, 5–7 March 2006, pp. 33–37.
[13] Tomlin, C., Pappas, G. J., and Sastry, S., "Conflict Resolution for Air Traffic Management: A Study in Multi Agent Hybrid Systems," *IEEE Transactions on Automatic Control*, Vol. 43, No. 4, April 1998, pp. 509–521.
doi:10.1109/9.664154
[14] De Francesco, N., and Massink, M., "Modeling Free Flight with Collision Avoidance," *Proceedings of the Seventh IEEE International Conference on Engineering of Complex Computer Systems* (ICECCS 2001), IEEE Computer Society, Washington, D.C., June 2001, pp. 270–279.
[15] Parastari, J., and Malaek, S. M., "Zero-Time-Delay Optimal Cooperative Tactical Maneuvers for Real Time Conflict Resolution in

ATM," *World Congress Aviation in the 21st Century*, National Aviation Univ., Kiev, Ukraine, 14–16 Sept. 2003, pp. 5.62–5.68.

[16] Jianghi Hu, Prandini, M., and Sastry, S., "Optimal Maneuver for Multiple Aircraft Conflict Resolution: a Braid Point of View," *Proceedings of the IEEE 39th Conference on Decision and Control*, Vol. 4, No. 4, Inst. of Electrical and Electronics Engineers, Piscataway, NJ, 2000, pp. 4164–4169.

[17] Tomlin, C., "Hybrid Control of Air Traffic Management Systems," Ph.D. Thesis, Dept. of Electrical Engineering & Computer Sciences, Univ. of California, Berkeley, Berkeley, CA, 1998.

[18] Dowek, G., Geser, A., and Minoz, C., "Tactical Conflict Detection and Resolution in a 3-D Airspace," NASA Langley Research Center, CR-2002-211637, Hampton, VA, 2001.

[19] Martin, D. A., and Willet F. M., "Development and Application of a Terminal Spacing System," Federal Aviation Administration, Rept. NA-68-25 (RD-68-16), Aug. 1968.

[20] Denery, D. G., and Erzberger, H., "The Center-TRACON Automation System: Simulation and Field Testing," NASA TM 110366, Aug. 1995.

[21] Davis, T. J., Krzeczowski K. J., and Bergh C., "The Final Approach Spacing Tool," *Proceedings of the 13th IFAC Symposium on Automatic Control in Aerospace*, Palo Alto, CA, Sept. 1994.

[22] Robinson J. E., and Isaacson D. R., "A Concurrent Sequencing and Deconfliction Algorithm for Terminal Area Air Traffic Control," *AIAA Guidance, Navigation, and Control Conference and Exhibit*, AIAA Paper 2000-4473, 14–17 Aug. 2000.

[23] Isaacson, D. R., and Robinson, J. E., "A Knowledge-Based Conflict Resolution Algorithm for Terminal Area Air Traffic Control Advisory Generation," *AIAA Guidance, Navigation, and Control Conference*, AIAA Paper 2001-4116, Montreal, Canada, 2001.

[24] Dubins, L. E., "On Curves with Minimal Length with a Constraint on Average Curvature and with Prescribed Initial and Terminal Positions and Tangents," *American Journal of Mathematics*, Vol. 79, 1957, pp. 497–516.
doi:10.2307/2372560

[25] Lindholm T. A. "Integrated Methods of Diagnosing and Forecasting Aviation Weather," *Proceedings of the 19th Digital Avionic System Conference*, Vol. 1, Inst. of Electrical and Electronics Engineers, New York, 2000, pp. 3D2/1–3D2/8.

[26] "General Operating and Flight Rules," *Code of Federal Regulations*, Title 14, Part 91, Federal Aviation Administration, 2002.

[27] Naderi E., "An Efficient Approach to Schedule Aircraft for Landing During Rush-Hour," M.Sc. Dissertation, Sharif Univ. of Technology, Tehran, Iran, 2008 (in Persian).

[28] Malaek, M. B., and Nabavi S. Y., "A General Approach in Optimal Management of Aircraft Landing in a Controlled Aerodome," 7th Conference of Iranian Aerospace Society, Tehran, Iran, Sharif Univ. of Technology Paper 309, 19–21 Feb. 2008 (in Persian).

[29] Holland, J. H., *Adaptation in Natural and Artificial Systems: An Introductory Analysis with Application to Biology, Control and Artificial Intelligence*, Univ. of Michigan Press, Ann Arbor, MI, 1975.

[30] McNealy, R. L., "Trajectory Planning for Micro Air Vehicles in the Presence of Wind," M.A. Thesis, Dept. of Mathematics and Statistics, Texas Tech Univ., Lubbock, TX, 2007.